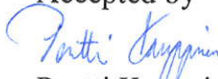**Groundwater + 100 mg/l S^{2-}**

Sulphide induced stress corrosion cracking of copper – Intermediate Report 3

Authors: Esko Arilahti, Taru Lehtikuusi, Timo Saario and Päivi Varis

Confidentiality: Public

Report's title	
Sulphide induced stress corrosion cracking of copper – Intermediate Report 3	
Customer, contact person, address	Order reference
KYT2010 Research Programme and SSM	
Project name	Project number/Short name
Sulphide induced stress corrosion cracking of copper	32986 / Cu SCC H2S
Author(s)	Pages
Esko Arilahti, Taru Lehtikuusi, Timo Saario and Päivi Varis	32
Keywords	Report identification code
copper, nuclear waste, stress corrosion cracking	VTT-R-10541-10

Summary

Precracked CT-specimens of CuOFP have been exposed to groundwater with 200 mg/l and 10 mg/l sulphide. On-line monitoring using the Potential Drop technique as well as displacement measurement of the specimen both indicated continuous changes in the material properties of CuOFP during the exposure. SEM/EDS studies of the fracture surface showed that during the exposure sulphur/sulphide had entered the material ahead of the precrack tip, with penetration rate of around 1 mm per week. Individual grain boundaries were found to contain above 20 a% sulphur. Optical metallography of sliced and polished cuts of exposed samples showed that sulphide inclusions could be found in all three dimensions of the material and not only in the crack plane. As a conclusion, the continuous changes in the on-line monitoring signals were attributed to the accumulation of sulphur/sulphide in the grain boundaries ahead of the precrack tip and further precipitation as inclusions.

Based on the results it is clear that sulphur can diffuse into the Cu OFP material when it is exposed at room temperature to saline groundwater with 10 to 200 mg/l sulphide. Indications were found that the in-diffusion preferentially occurs through grain boundaries and that high stress favours accumulation of sulphur/sulphide. Further investigations are needed to determine the effects of sulphur/sulphide indiffusion on mechanical properties of CuOFP.

Confidentiality	Public

Espoo 10.1.2011

Written by	Reviewed by	Accepted by
Timo Saario	Petri Kinnunen	Pentti Kauppinen
Chief Research Scientist	Team Manager	Technology Manager

VTT's contact address

P.O.Box 1000, FI-02044 VTT, Finland

Distribution (customer and VTT)
SSM / Jan Linder 1 copy, VTT 1 copy

Preface

This Intermediate Report covers the progress made in the KYT2010 –research program project "Sulphide induced stress corrosion cracking of copper" between January 22 and 30 December, 2010.

Espoo 14.1.2011

Authors

Contents

1   Introduction

Copper canister is a central technical barrier for radioactive release from high level nuclear waste. Stress corrosion cracking (SCC) is a failure mechanism which has the potential capacity of damaging all the canisters in a relatively short time.

In 2007 a new Japanese research showed that also sulphide (S^{2-}) can cause SCC in pure copper under anoxic high chloride water conditions /1/. Sulphides may come to contact with the copper canister surface through three different processes: 1) transport via groundwater flow, 2) production at the bentonite/rock interface via sulphate reducing bacteria (SRB) and further transport and 3) through SRB activity within bentonite (pyrite reduction). In the groundwater sulphide concentrations are typically relatively low, 1-3 mg/l. The maximum value that can be formed through SRB activity at the bentonite/rock interface is not exactly known, but can be high, causing a high diffusion gradient through the bentonite. The sulphide concentration that forms because of SRB activity within bentonite is known to some extent as a function of bentonite density. According to experimental findings sulphides form within the bentonite even in fully compacted bentonite /2/. In scenarios where the density of bentonite locally decreases (e.g. piping, erosion-corrosion) the access of sulphide to the copper surface will be much easier.

2   Goal

The goals of the project are to evaluate the sulphide induced SCC risk of copper canisters under repository conditions. Technical targets are:

1.   Develop an experimental arrangement for SCC tests in sulphide containing groundwater.

2.   Determine experimentally the minimum concentration of sulphide in groundwater which can cause SCC in pure copper (CuOFP).

3.   Evaluate the maximum sulphide concentration which can form at the bentonite/rock interface because of SRB activity.

4.   Develop a diffusion model and make a quantitative estimate of the sulphide concentration reaching the surface of the copper canister in three different scenarios.

3   Results

In the following results in relation to technical targets 2 and 4 (above) gained between January 22 and December 30, 2010 are presented. Earlier results have been reported in the following reports: Sulphide induced stress corrosion cracking of copper – Intermediate Report 1 (VTT-R- 07999-09), Sulphide induced stress

corrosion cracking of copper – Intermediate Report 2 (VTT-R-00652-10), Sulphide induced stress corrosion cracking of copper – the effect of SRB activity (VTT-R-09242-09) and Diffusion model for sulphide in compacted bentonite (VTT-R- 00662-10).

4 Task 2. Determination of the minimum sulphide concentration causing SCC in CuOFP

The research method used is the constant load method with so-called Compact Tension (CT) –test piece, where the stress-strain state forming at the crack tip corresponds to the multiaxial stress-strain in the copper canister. A prefatigue crack was made in the test piece by high cycle fatigue in air.

The base electrolyte used was the saline groundwater corresponding to Olkiluoto groundwater (Table 1). The sulphide was added as Na_2S. Before the sulphide addition the pH of the base solution was increased to pH = 9 by NaOH to prevent the formation of H_2S during the following sulphide addition.

Table 1. The *composition of the saline reference groundwater in anoxic condition*

Element	Concentration	
	mg/l	mmol/l
Na^+	4800	208.8
K^+	21	0.54
Ca^{2+}	4000	100
Mg^{2+}	54.6	2.3
Sr^{2+}	35	0.4
B^{3+}	0.92	0.08
SO_4^{2-}	4.2	0.044
Cl^-	14500	412.7
F^-	1.2	0.063
Br^-	104.7	1.31
I^-	0.9	0.007
pH	8.2	

4.1 Test run 4 with 10 mg/l S^{2-}

The test run was performed with a target level of 10 mg/l sulphide. During the test the sulphide level and pH were measured regularly, see Fig. 1. Sulphide measurement was performed with ampules (CHEMetris VACUettes Kit K-

9510D), which results in an accuracy of about ±0.5 mg/l of sulphide. The pH was measured with Thermo scientific Orion 5 Star Benchtop meter. Despite of covering most of the surface of the CT-specimen with lacquer, the sulphide level was found to be decreasing as a function of time so that regular refilling was needed. The level was restored each day to about 10 mg/l by adding groundwater with 387 mg/l sulphide (storage electrolyte). The average level of sulphide during the test was 8.6 mg/l.

Because of hydrolysis of Na_2S through the reaction

$$S^{2-} + H_2O = SH^- + OH^- \qquad (K_b \sim 8{,}3)$$

the addition of sulphide produces an increase of pH. In an otherwise unbuffered system addition of 10 mg/l sulphide should result in a pH of 10.5. Thus, the measured pH roughly agrees with the measured sulphide concentration.
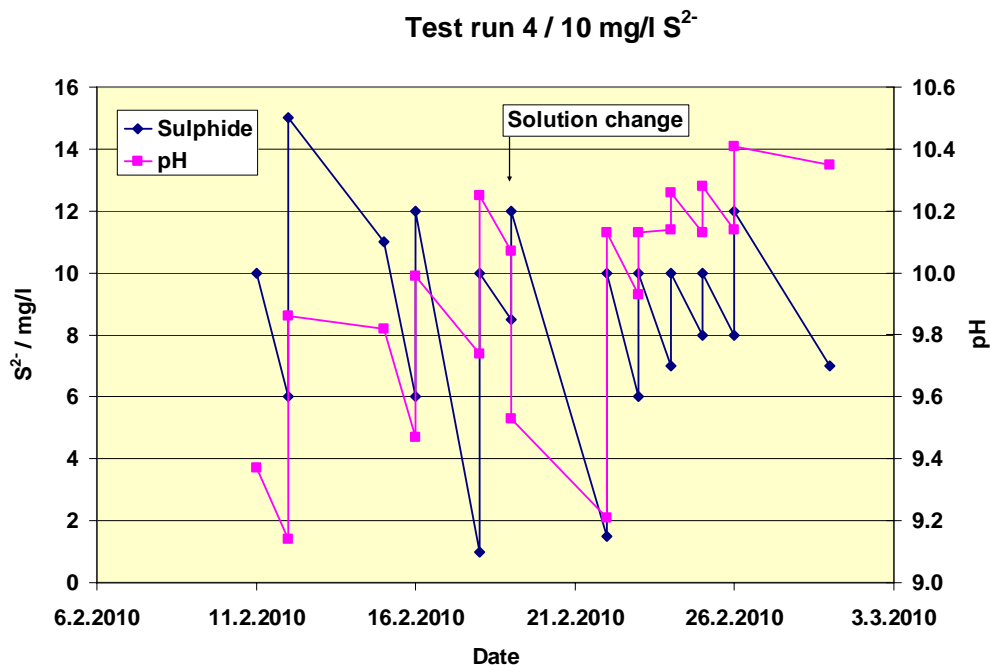

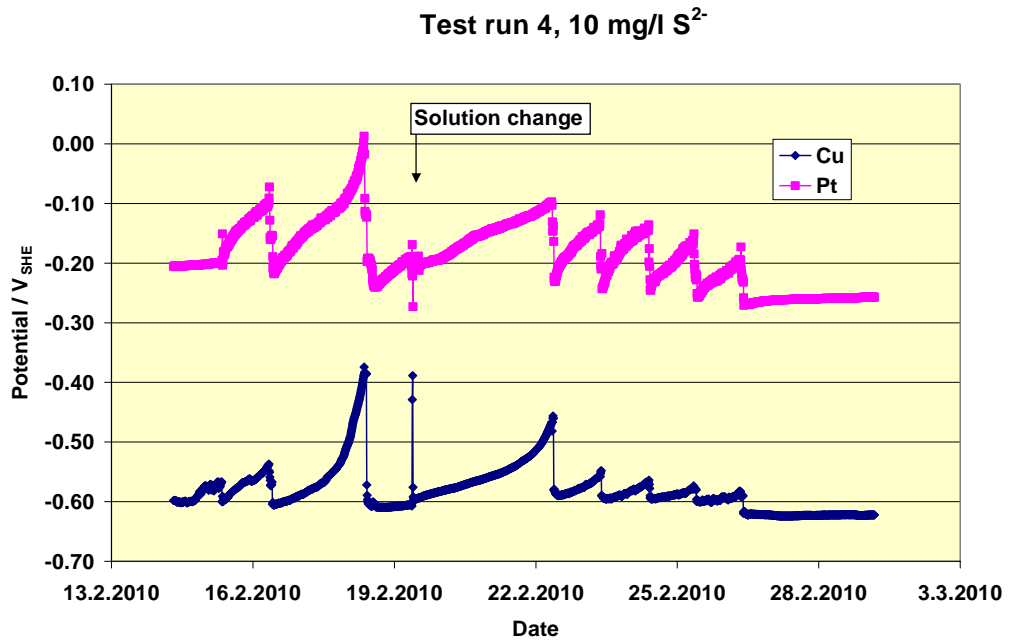Figure 1. Sulphide concentration and pH as a function of test duration.

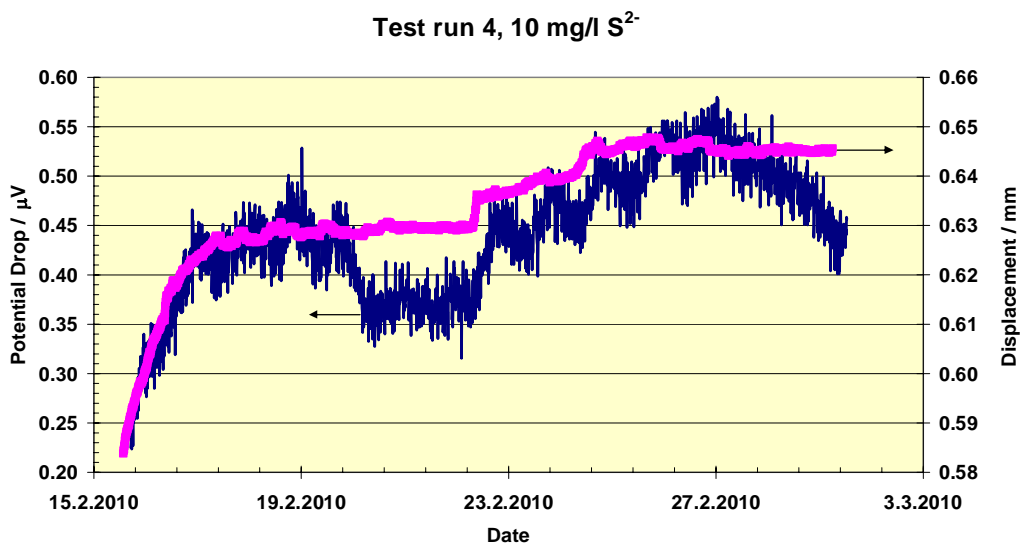Figure 2. Potential of Cu-specimen and Pt-plate as a function of test duration.

Figure 3. Potential Drop –signal and displacement of the test piece as a function of time.

The potential of the Cu-specimen and Pt-plate (redox-potential) are shown in Fig. 2. The Cu-specimen potential is about $E_{Cu} = -0.6$ V_{SHE} during most of the test period, increasing somewhat as sulphide concentration decreases, and returning to the original value as sulphide concentration is replenished. Potential of Pt-plate (the redox-potential) is between -0.25 $V_{SHE} < E_{Pt} < -0.15$ V_{SHE} for most of the test period, also following the sulphide concentration.

The Potential Drop-signal (indicating electrical resistance of the test piece) and the displacement of the CT-specimen show a small increase during the test period, indicating some process changing the properties of the CuOFP-material ahead of the crack tip. Displacement measures the opening of the CT-specimen, and is affected by the initial loading and following time dependent processes such as creep and/or crack growth. An increase of the crack length during the test will result in a decrease of the cross sectional area of the test piece, which again is detected as an increase of the electrical resistance (in practise as an increase of the Potential Drop –voltage signal).

In fracture mechanical terminology, the loading used corresponds to a stress intensity of about $K_I = 9$ MPam$^{1/2}$.

After test termination the fracture surfaces were examined with both optical and scanning electron microscopy (SEM). The test piece showed an extensive share of grain boundaries in the fracture surface already within the air fatigue area as shown in Fig. 4. This is similar to all of the test pieces, and thus the fracture surface appearance can not be used to determine whether SCC has taken place during the test.
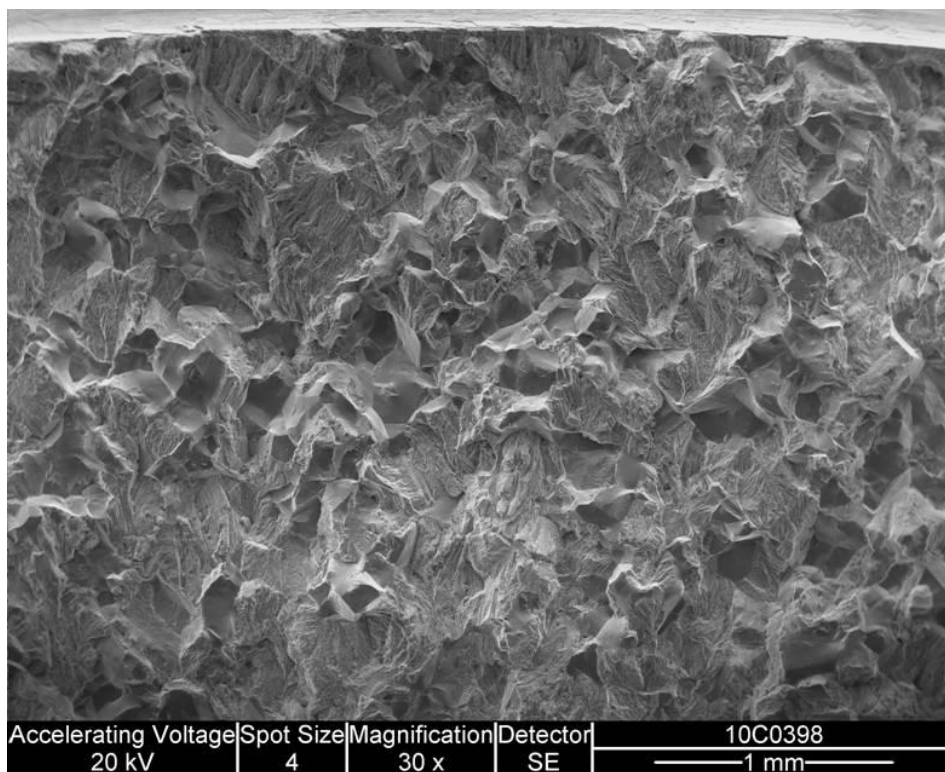

Figure 4. SEM-picture of the prefatigue area. The upper most detail is the machined notch tip.

4.2   Test run 5 with 200 mg/l S^{2-}

The fifth test run was performed with a higher sulphide level of S^{2-} = 200 mg/l.
Fig. 5 shows the pH and sulphide concentration as a function of test duration. The
pH on average increases slightly during the test run, as a result of sulphide
hydrolysis. In Fig. 6, the potentials of Cu and Pt are shown to be rather stable and
at a reasonable level. The displacement of the specimen shows a continuous slow
increase throughout the test duration, as does the Potential Drop-signal, Fig. 7. As
discussed above in case of the test run 4, an increase of these parameters is an
indication of some process changing the properties of the CuOFP-material ahead
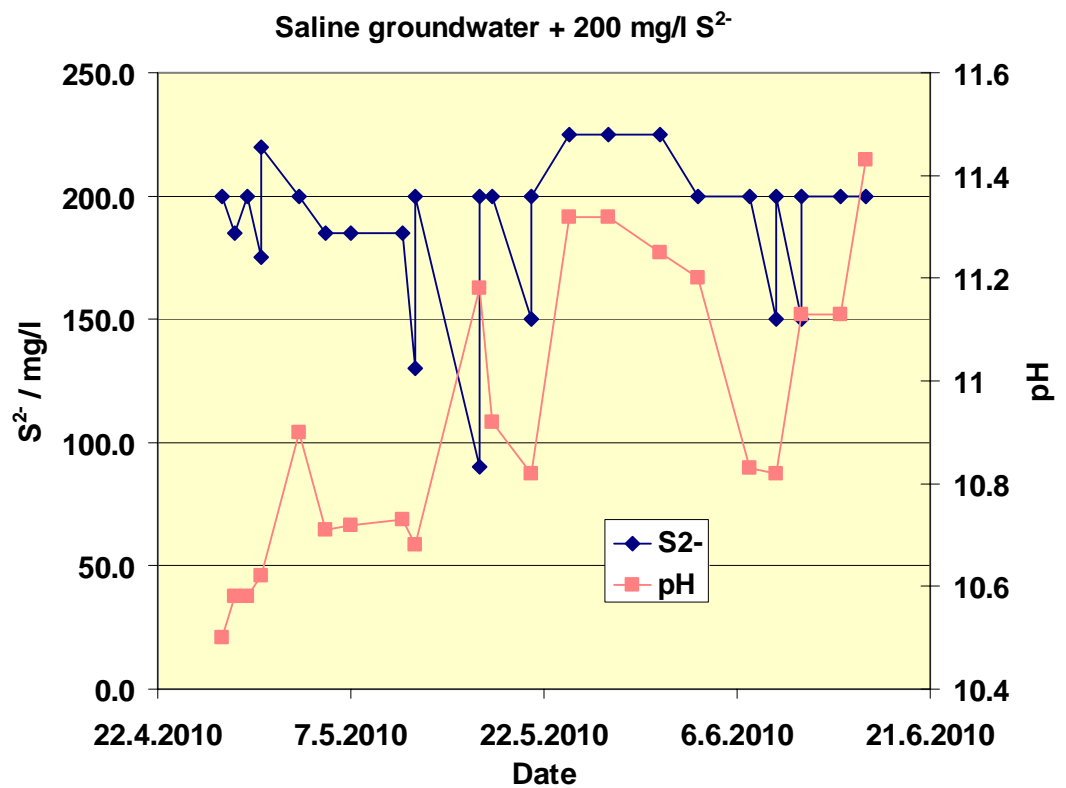of the crack tip.

Figure 5. Sulphide concentration and pH as a function of test duration, Test run 5.
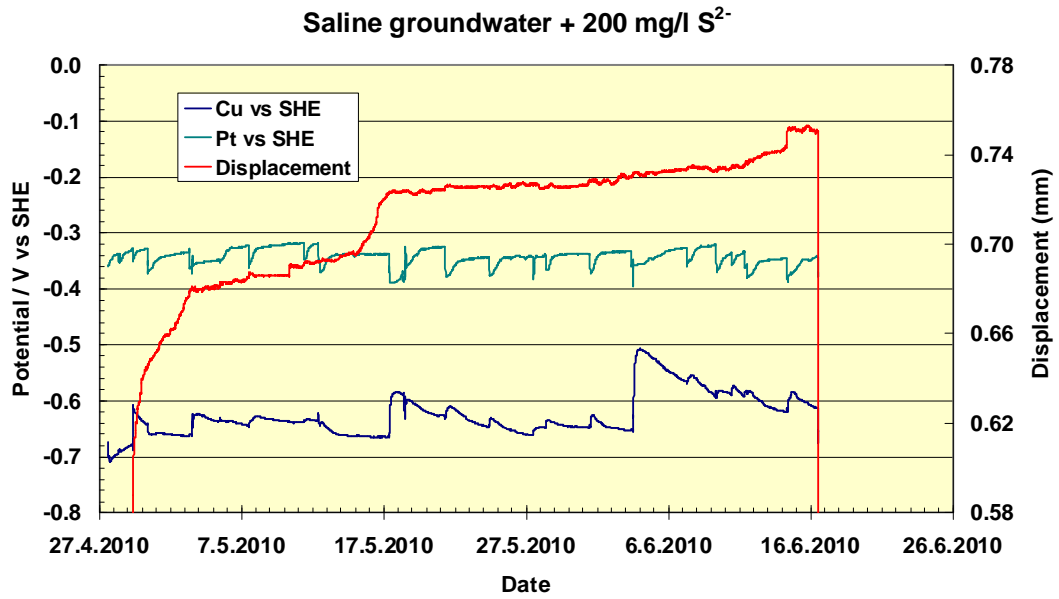
Saline groundwater + 200 mg/l S²⁻

Figure 6. Potentials and displacement (crack opening) of the test piece as a function of time, Test run 5.
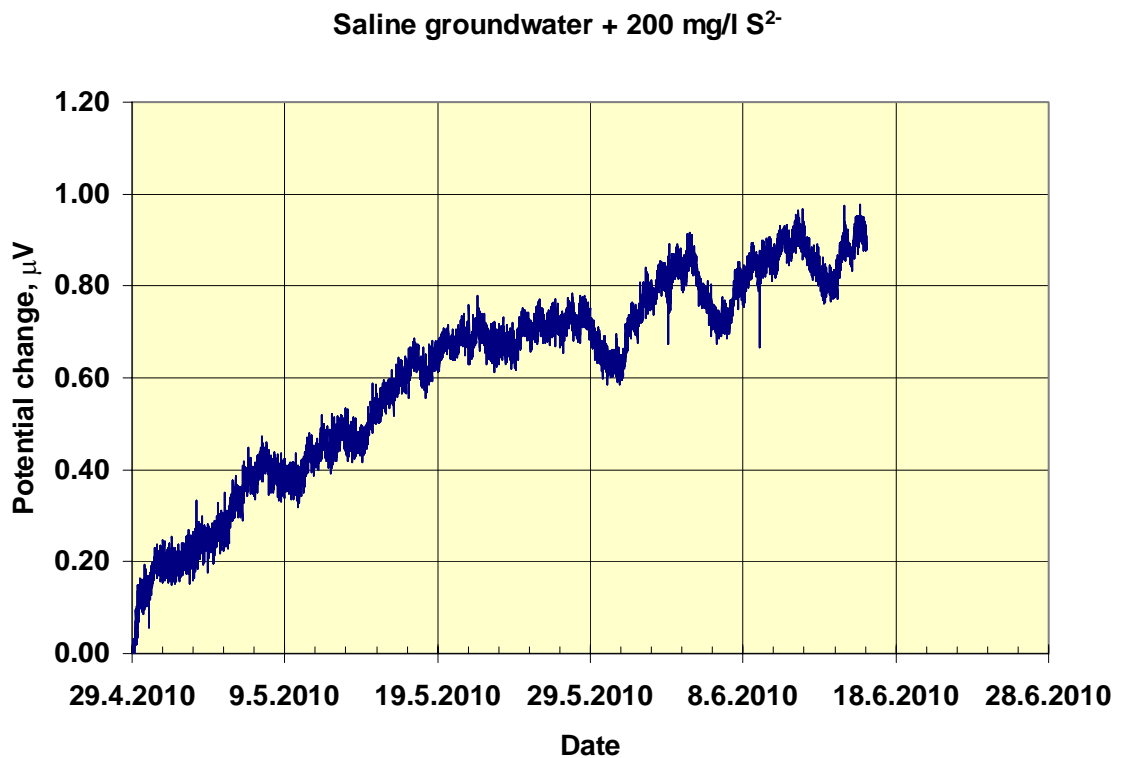
Saline groundwater + 200 mg/l S²⁻

Figure 7. Potential Drop –signal of the test piece as a function of time, Test run 5.

After the exposure period the specimen was first partially cut mechanically from the back side of the specimen along the precrack surface line to prevent extensive

plastic deformation during afterfatigue. Next, the specimen was fatigued in air until fracture occurred. The fracture surface of the specimen revealed by further fatigue (Figs 8 and 9) showed that the prefatigue area was covered with black surface layer (copper sulphide). The after-fatigue area (number 2) showed black spots and/or black areas several millimetres ahead of the crack tip, i.e. in material which was not directly exposed to the environment.

A compositional analysis of a representative part of the area (Fig. 10) with SEM/EDX showed 58.7 at% Cu and 22.5 at% S. This indicates that a considerable part of the exposed grain boundaries are covered with a sulphide film. Fig. 10 shows a comparison of normal and backscattered SEM images of a representative area ahead of the crack tip, revealing that there are some particles which seem like precipitates, and that also most grain boundaries that are perpendicular to the fracture surface contain of a lighter phase, presumably a Cu-S-precipitate. Spot analysis of a single grain boundary in this area showed basically only Cu and S. Some but not all of the particles were identified as Cu-S-precipitates. It is assumed that the increase of the PD-signal during the exposure (see Fig. 7) is caused by formation of sulphide films on grain boundaries and sulphide inclusions ahead of the crack tip. Copper sulphide is a poor electrical conductor compared to copper. Thus, the formation of copper sulphide ahead of the crack tip is seen as an average increase of electrical resistance of the load bearing cross sectional area of the specimen, i.e. as an increase of the PD-signal.
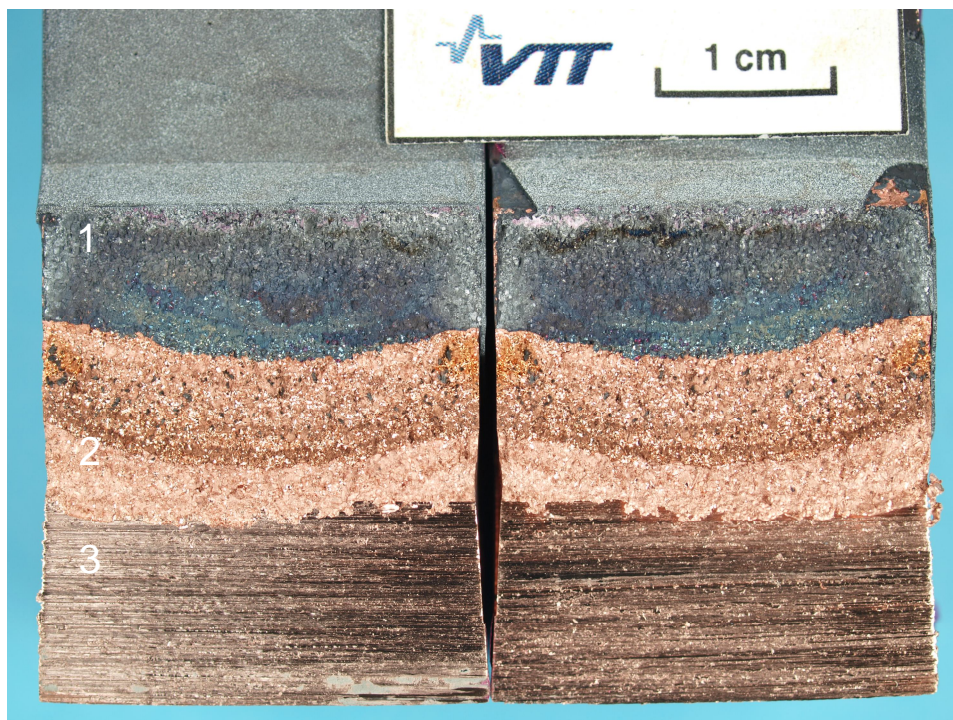

Figure 8. A digital image of the two sides of the fracture surface. s, red lines marking the crack extension during exposure. Number 1 refers to the prefatigue area next to the machined notch, number 2 to the afterfatigue area and 3 to the area mechanically cut from back side of the specimen to prevent extensive plastic deformation during afterfatigue.
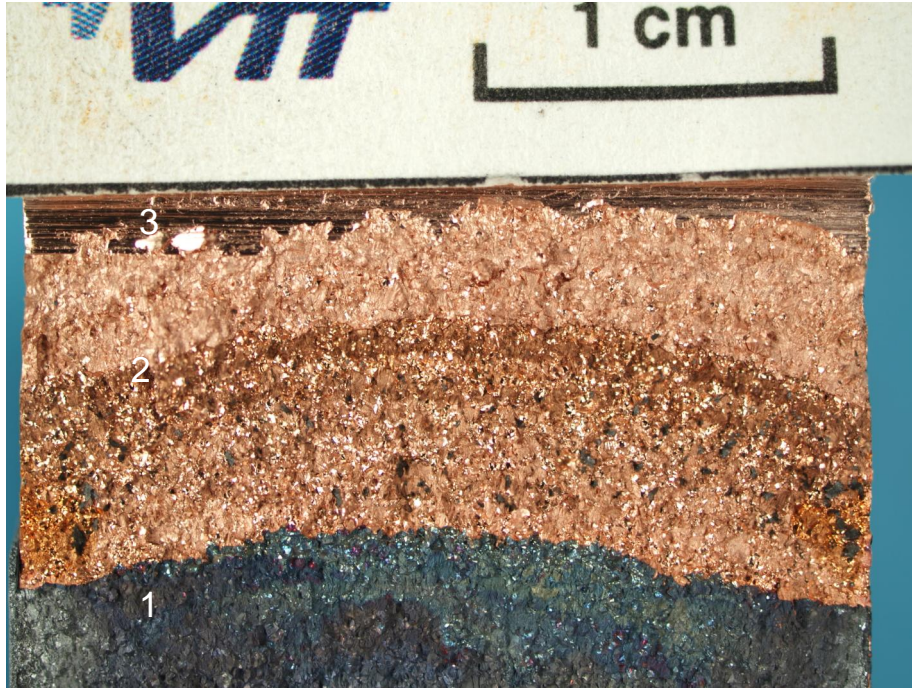
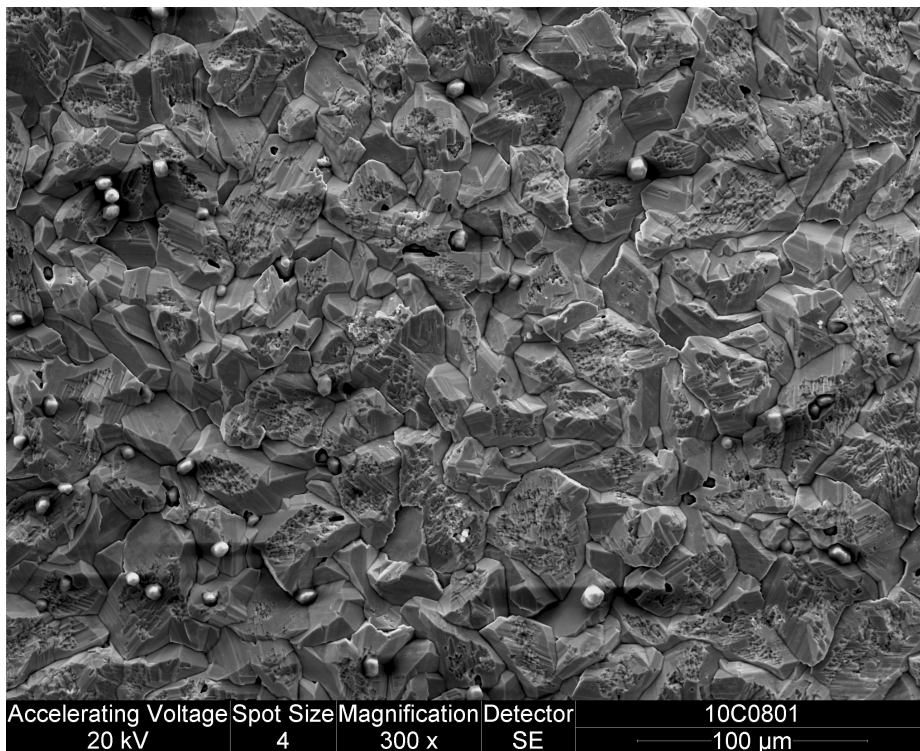Figure 9. A close-up of the surface shown in Fig.8.

| Accelerating Voltage | Spot Size | Magnification | Detector | 10C0801 |
| 20 kV | 4 | 300 x | SE | 100 µm |

Figure 10a. SEM-picture of the after-fatigue area.

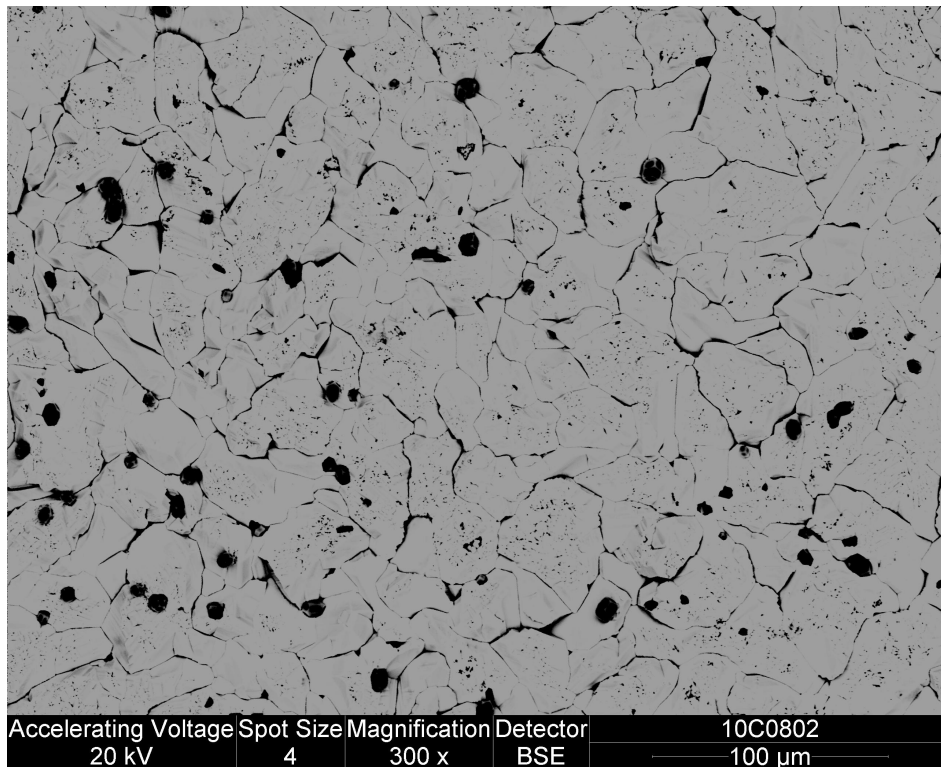| Accelerating Voltage	Spot Size	Magnification	Detector	10C0802
20 kV	4	300 x	BSE	100 µm

Figure 10b. The same area as in Fig. 10, in BSE -mode.

4.3   Test run 6 in N_2/air

A test run was made using exactly the same testing sequence and equipment as before but instead of exposing the sample to groundwater with sulphide the pressure vessel was filled with nitrogen gas. Exposure time was two weeks. No continuous change in the Potential Drop signal was detected, as expected, Fig. 11.
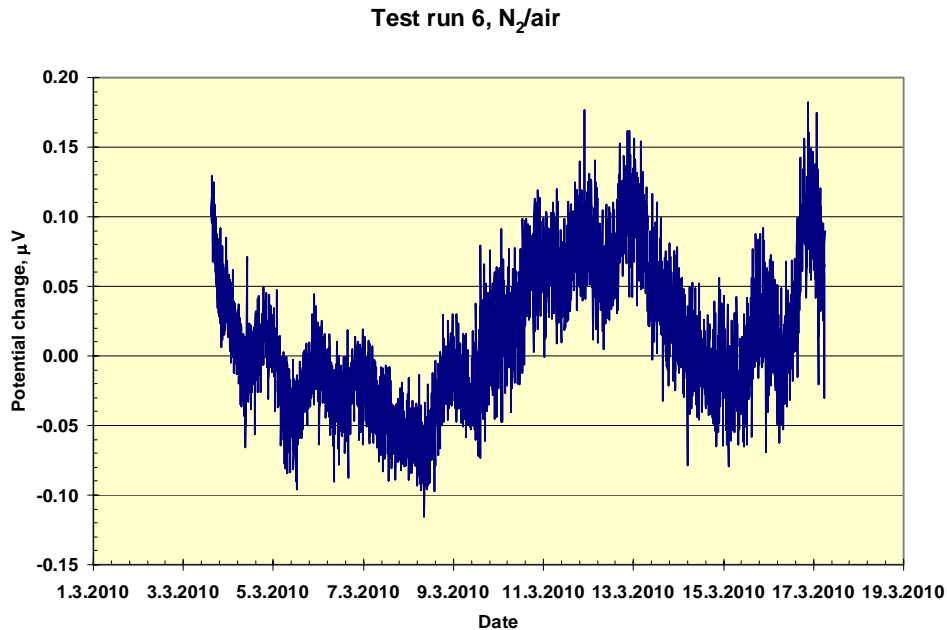
Test run 6, N$_2$/air

Figure 11. Potential Drop –signal of the test piece as a function of time, Test run 6 (N$_2$/air).

Fig. 12a shows the fracture surface (produced by afterfatigue) and Figs 12b and 12c SEM pictures of the different parts of the surface. The percentage of grain boundaries on the fracture surface is very high both in the prefatigue and afterfatigue areas. The test was performed to verify that both the prefatigue and afterfatigue procedures produce a fracture surface with a considerable portion of grain boundaries without the presence of the groundwater environment. Thus, the presence of grain boundaries on the fracture surfaces could not be used as an indication of SCC in case of CuOFP. The reason why the fatigue procedure is able to drive the fatigue crack along the grain boundaries is unclear. The SEM/EDS analysis of the grain boundary areas for this sample showed only Cu and O. Thus, at least severe segregation of P into the grain boundaries as a possible cause of weakening the adhesion of the grain boundaries could be ruled out.

Figure 12a. A digital picture of the fracture surface, Test run 6 (N_2/air). The prefatigue area (1) and afterfatigue area (2).
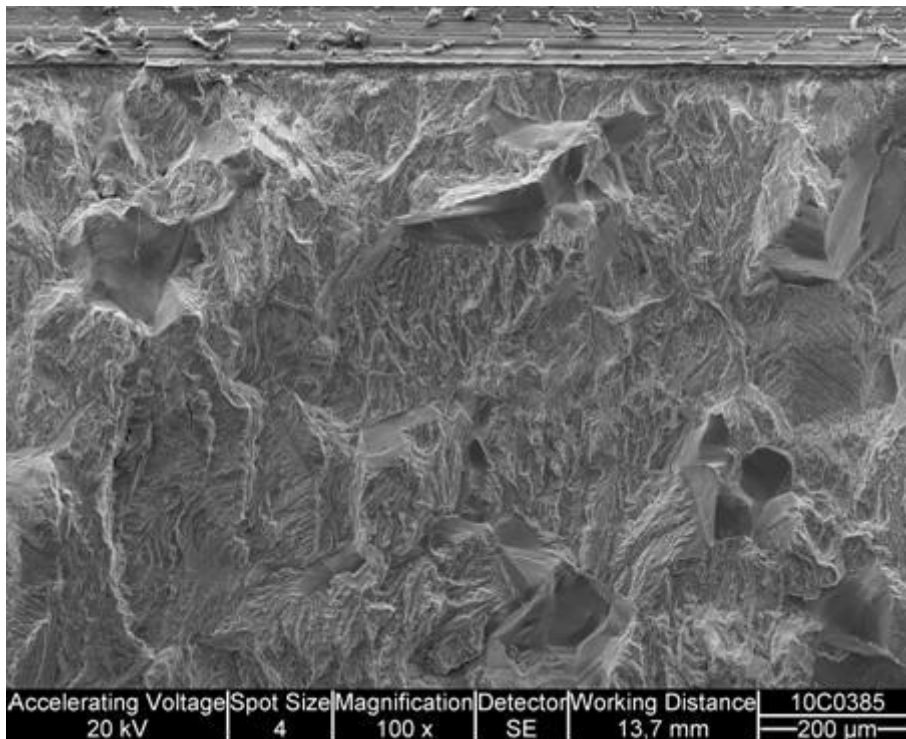

Figure 12b. SEM-picture of the prefatigue area, with the machined notch at the upper edge of the picture. Test run 6 (N_2/air).
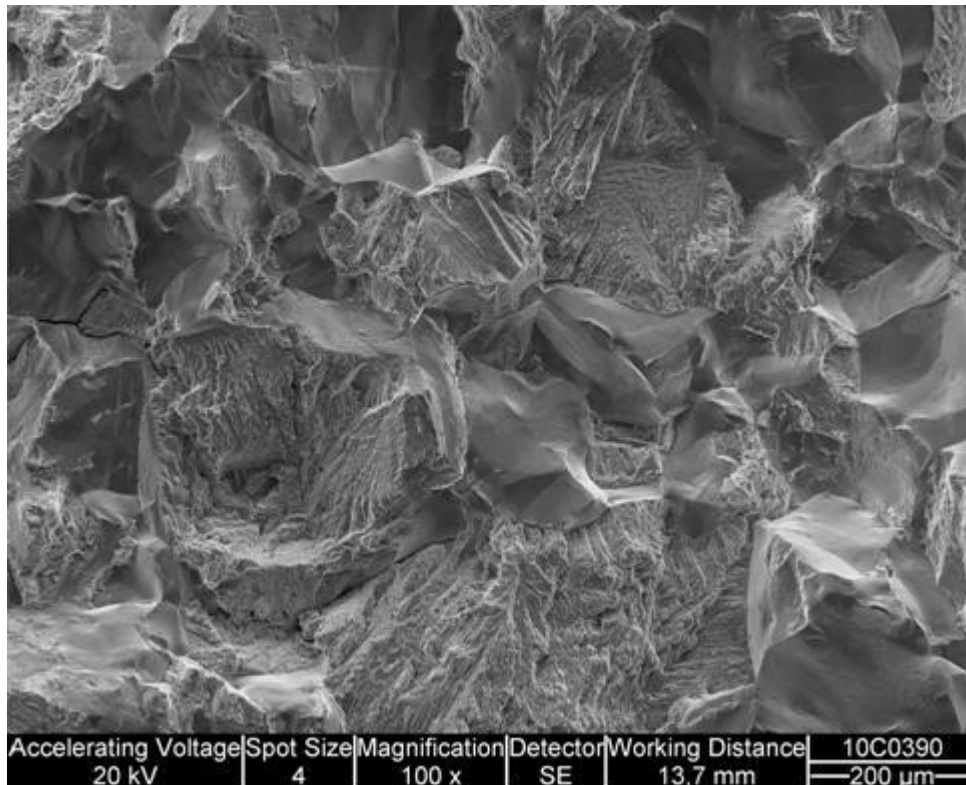
Figure 12c. SEM-picture of the start of the afterfatigue area. Test run 6 (N_2/air).

4.4   Test run 7 and 8 in groundwater with 200 mg/l S^{2-}

In this test run, one specimen (Nr 7) was kept in the environment (groundwater with 200 mg/l S^{2-}) but not loaded, while another specimen (Nr 8) was loaded to the same loading level, i.e. $K_I = 9$ MPam$^{0.5}$, as the previous specimens. At the end of the test period the load was increased slightly for a period of three days, in order to test the effect of additional mechanical loading.

The potentials of Cu and Pt, Fig. 13, were found to be very similar to the Test run 5 in a similar environment. The displacement of the specimen showed also a similar, continuously growing trend, with a large increase as a response to the increase in load at the end of the period, Fig. 14. The increase in displacement due to the load increase was about double to the one in Test run 1 (with 100 mg/l S^{2-}), which may indicate deterioration of the mechanical properties of CuOFP due to in-diffusion of sulphur.

The Potential Drop –signal showed only a small increase during the test period, with a relatively high increase as a response to the increase in load, Fig. 15. SEM/EDS analysis of the area ahead of the crack tip showed again considerable portion of grain boundaries, Fig. 17. The EDS area analysis on five areas at different locations ahead of the crack tip showed sulphur concentrations between

21 and 28 a%, indicating an almost total coverage of the fracture surface by copper sulphide.
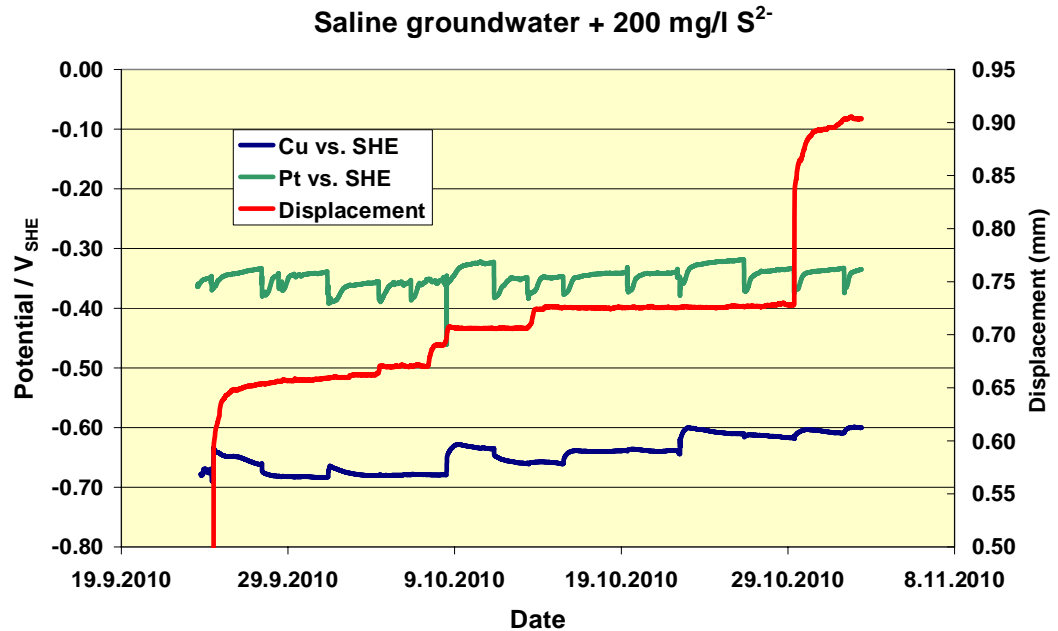

Figure 13. Potentials and displacement (crack opening) of the specimen 8 as a function of time, Test run 7/8 (specimen 7 was not loaded and not monitored).
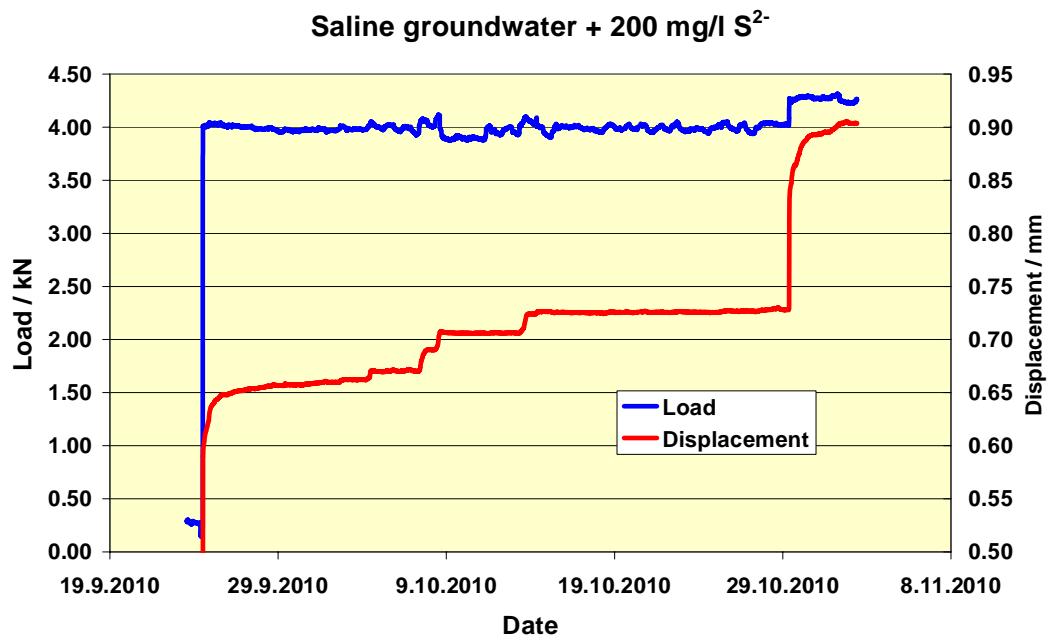

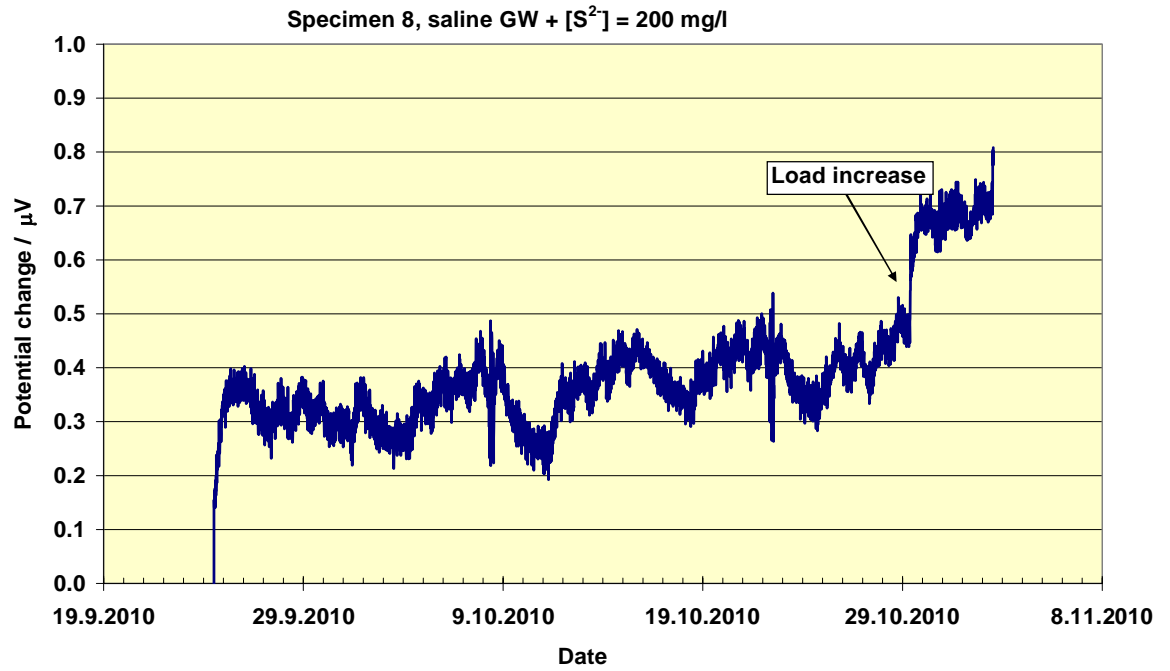Figure 14. Load and displacement as a function of time, specimen 8, Test run 7/8.

Figure 15. Potential Drop –signal of the test piece as a function of time, Test run 7/8.

Figure 16. Fracture surface of specimen 8 after the exposure, showing black spots ahead of the crack tip. Prefatigue (1) and afterfatigue (2) areas. Test run 7/8, specimen 8 (loaded).
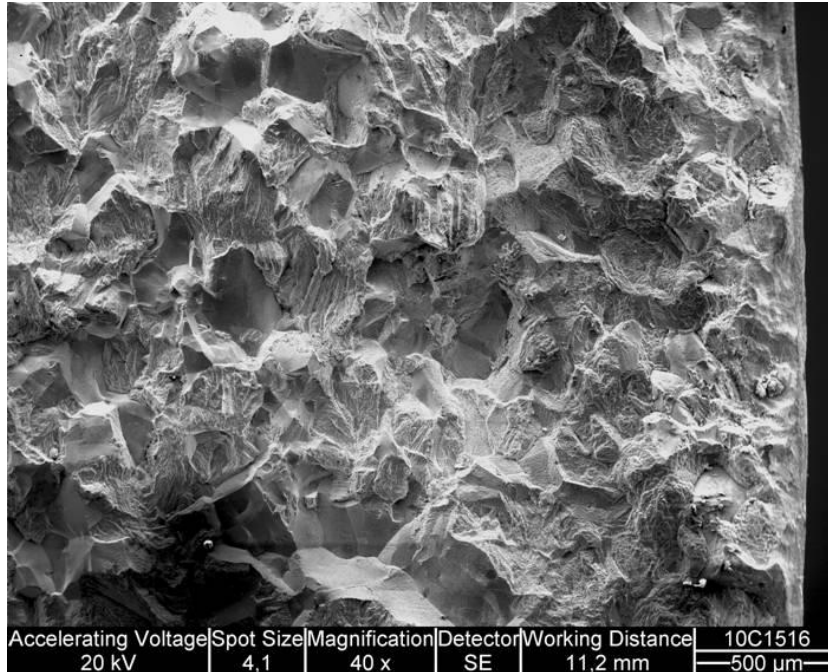
Figure 17. SEM-picture of the start of the afterfatigue area. Test run 7/8, specimen 8 (loaded).
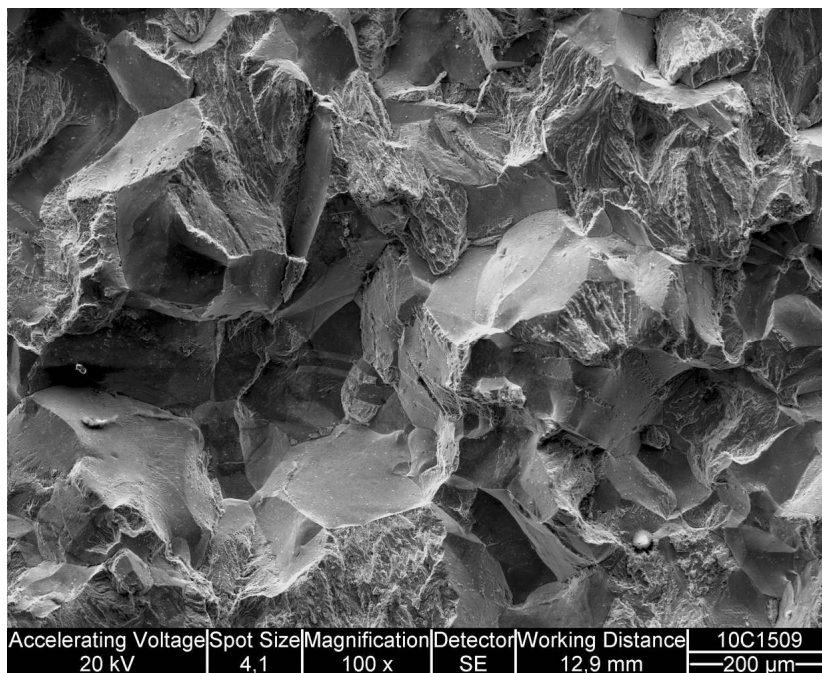

Figure 18. SEM-picture of the start of the afterfatigue area. Test run 7/8, specimen 7 (unloaded).

Fig. 18 shows the general appearance of the unloaded specimen (nr 7) in the after-fatigue area ahead of the crack tip with considerable portion of grain boundaries. The EDS area analysis on five areas at different locations ahead of the crack tip showed sulphur concentrations between 9 and 26 a%, slightly lower concentrations than in the case of the loaded specimen (Nr 8). This tends to indicate that stress (loading) increases the rate of in-diffusion of sulphur into CuOFP.

4.5 Additional analysis of Test run 1

After realising that sulphur has a tendency for in-diffusion into CuOFP, the specimen Nr 1 from test run 1 was taken under more detailed study. For this specimen, no lacquer was used so the whole specimen surface was in direct contact with the groundwater. A careful examination of the fracture surface (Fig. 19) reveals that also here black spots are present ahead of the crack tip but to a much smaller degree than in the case of the specimens exposed to groundwater with 200 mg/l S^{2-} (i.e. samples 5 and 8 above).

In the first phase, SEM/EDS analysis was performed in a more continuous way. Area analysis on the fracture surface ahead of the crack tip was performed along two red dashed lines (see Fig. 19), the distance between two adjacent areas chosen as 1 mm. The first line of analysis was located at about 2 mm from the left hand side of the specimen and extended 10 mm away from the crack tip. The second line of analysis was located at about 2 mm distance ahead of the crack tip and extended from about 2 mm distance from the side towards the centre of the specimen. The sulphur concentration (at%) decreased as a function of distance along both lines, see Fig. 20. The concentration profiles are not typical diffusion profiles, and a more detailed modelling effort would be needed to estimate e.g. the diffusion coefficient of sulphur/sulphide from these profiles.
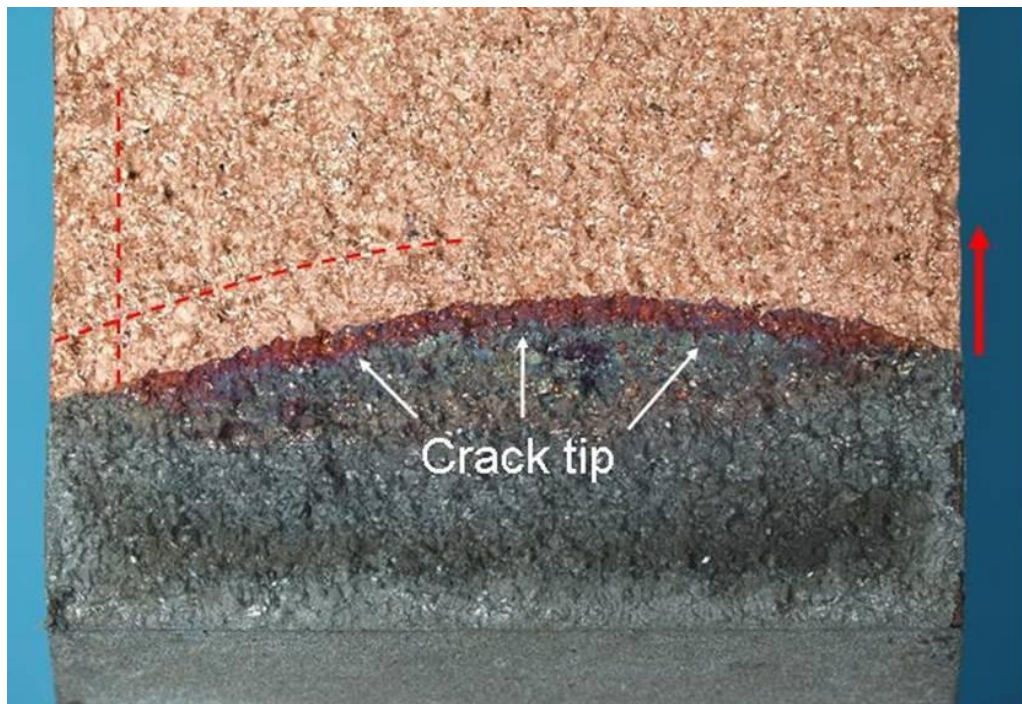

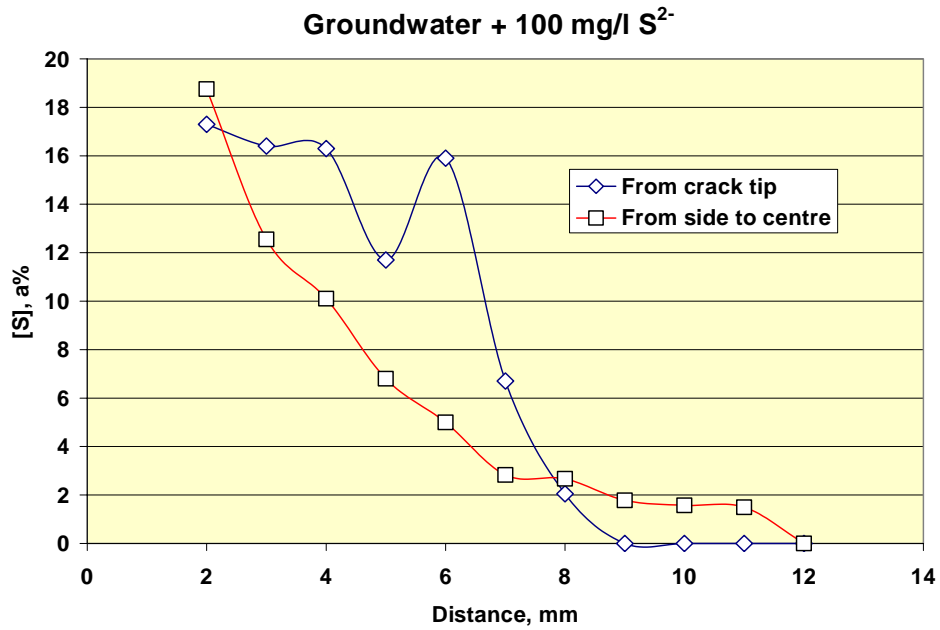Figure 19. Fracture surface of specimen Nr 1 (tested in groundwater with 100 mg/l S^{2-}).

Figure 20. Sulphur concentration (at%) on the fracture surface of specimen Nr 1 (tested in groundwater with 100 mg/l S^{2-}) as found by SEM/EDS -analysis.
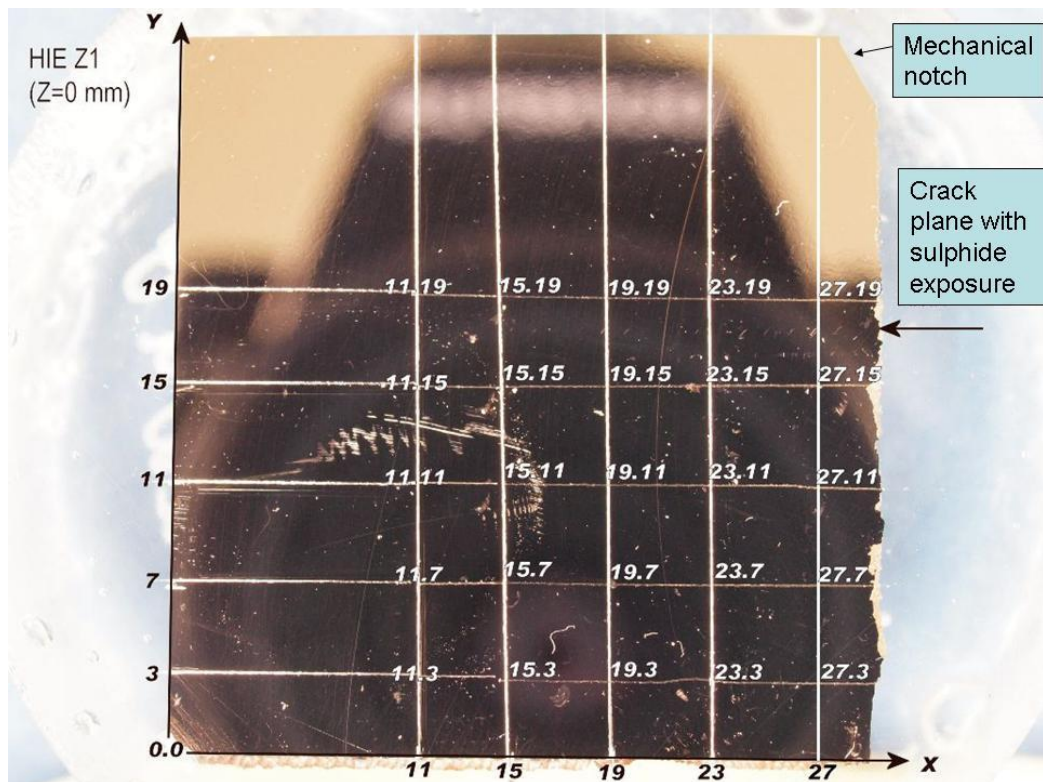

Figure 21. Slice Z1 of specimen Nr 1.

To further determine the extent of in-diffusion in specimen Nr 1, the specimen was sliced to reveal four separate planes ahead of crack tip and perpendicular to the crack plane (see Fig. 21). Here Z is the distance from the side towards the centre of the specimen. Thus, Z = 0 mm indicates that this surface is the outer surface of the specimen. The X and Y are the coordinates according to which digital images were taken with light microscope and further analysed with Image J –software to provide a particle area fraction and size distribution analysis of the sulphide inclusions. An analysis was performed for the X and Y coordinates of every cross section, i.e. 25 analyses for one slice. The other three slices had Z coordinates Z2 = 4 mm, Z3 = 8 mm and Z4 = 12 mm. Thus, slice Z4 would represent the material right at the centre of the specimen.

As an example of the images, Fig. 22 shows a comparison of unexposed CuOFP and the cross section 27.11 in Fig. 21. Based on such a comparison, it is safe to assume that all inclusions found (at this magnification) are in fact sulphides. In the Image J –analyses, the lower limit was set to 1 μm^2, i.e. about one pixel. Using the same criteria for the unexposed sample shown in Fig. 22 below resulted in no indications.

Figure 22. Comparison of polished surface of unexposed CuOFP and that of cross section 27.11 of slice Z1 in Fig. 21. Area fraction of inclusions is $6.5*10^{-4}$.

Figure 23. Area fractions of inclusions ($\times 10^4$) in slice Z1 (0 mm from outer surface) as a function of location.

Figure 24. Area fractions of inclusions ($\times 10^4$) in slice Z2 (4 mm from outer surface) as a function of location.
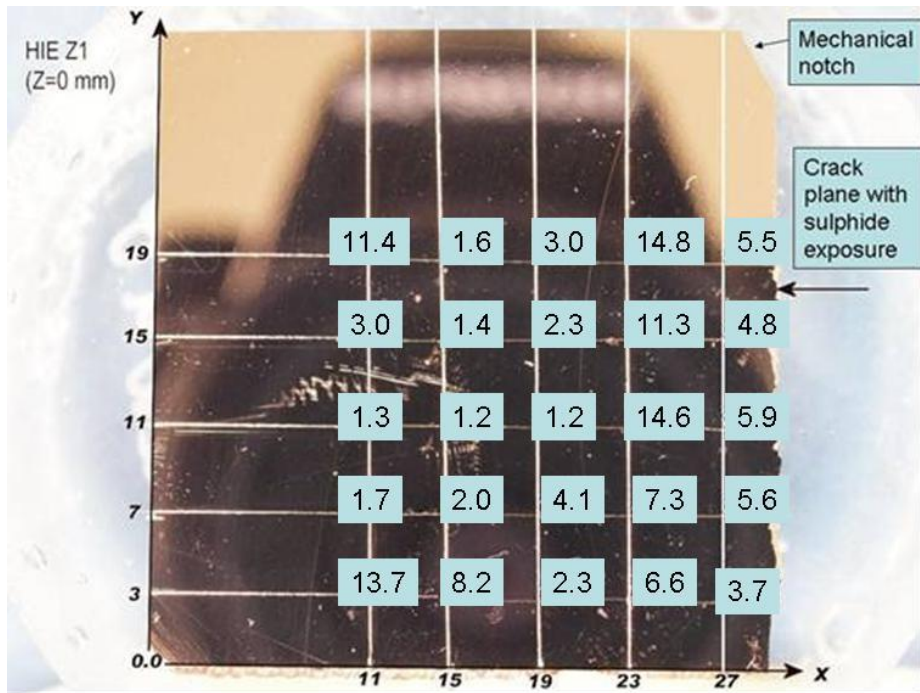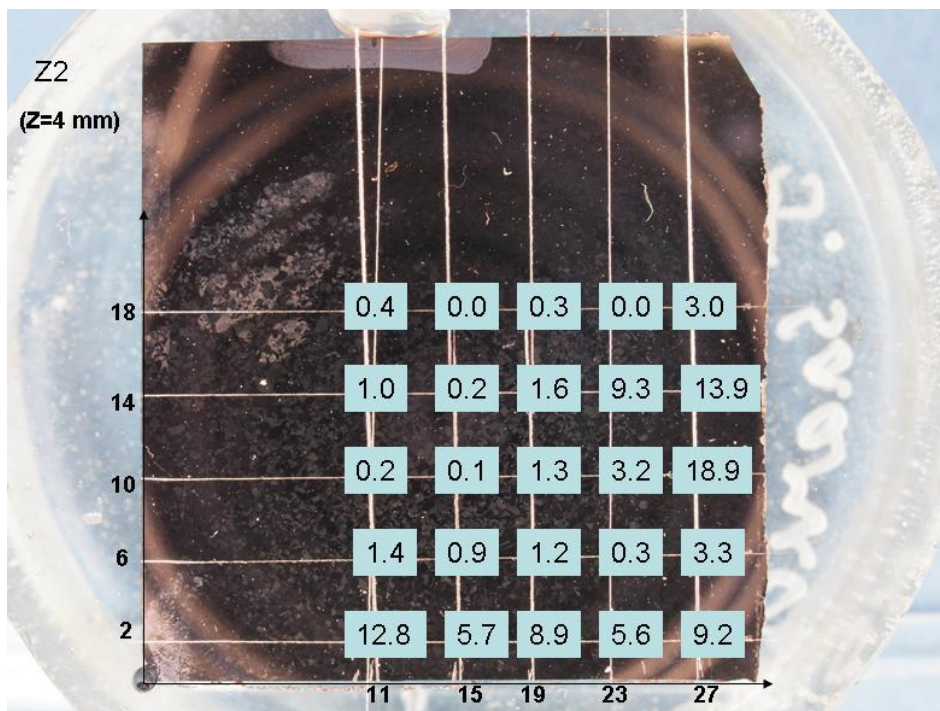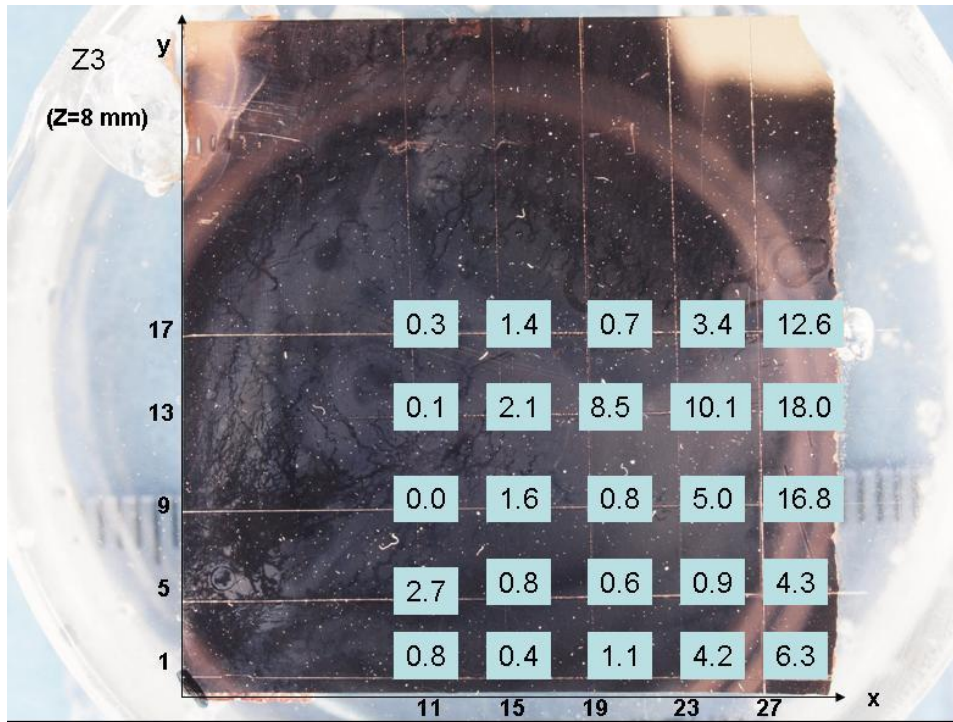
Figure 25. Area fractions of inclusions ($\times 10^4$) in slice Z3 (8 mm from outer surface) as a function of location.
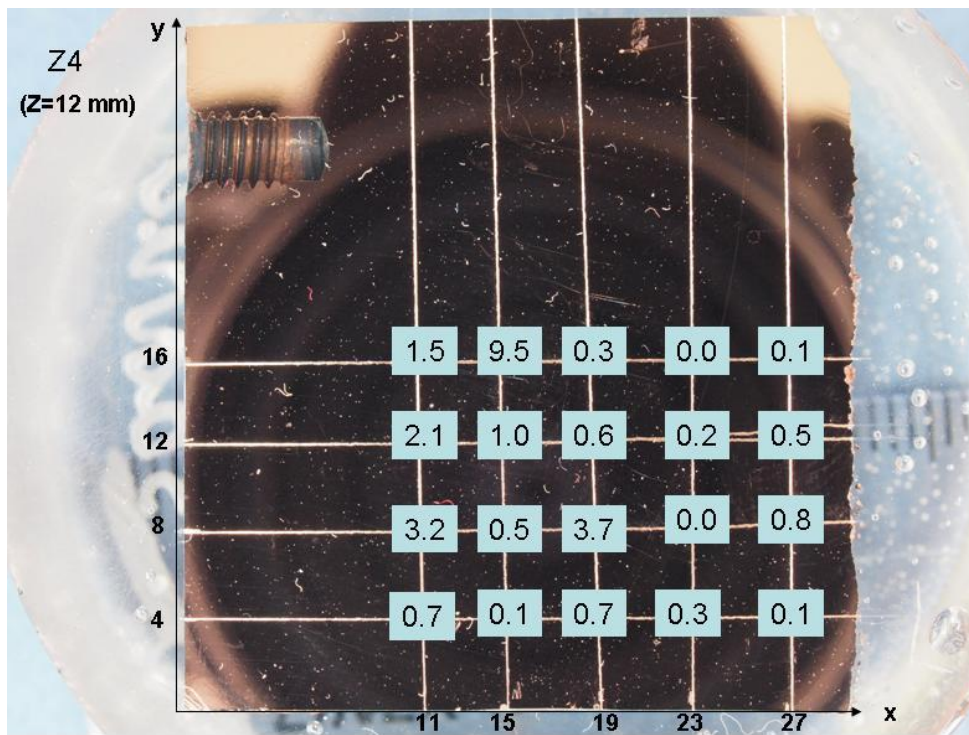

Figure 26. Area fractions of inclusions ($\times 10^4$) in slice Z4 (12 mm from outer surface) as a function of location.

Figures 23 to 26 show the area fraction of inclusions found on the different slices as a function of location on each slice. The analysed area at each location was 3.6 mm^2. The inclusion size (average for each location analysed) varied between 1.7 and 66 μm.

When looking through the data in Figs 23 to 26 one may wish to keep in mind the distance of different locations to the source of sulphur, the groundwater. For example, in case of slice Z1, i.e. the outer surface of the specimen, sulphur has had access to all of the surface locations directly. Thus, one would expect to find high values at practically all the locations. In practise, inclusions were found at all analysed locations, although there seems to be a very high variability on the area fraction. Going deeper into the material one would expect to find less inclusions at the locations farthest from the source, e.g. at location x=11 y=18 in Fig. 24 and x=11 y=17 in Fig. 25. This is also roughly in line with the actual results. As expected high area fractions are found closer to the fracture plane (i.e. along the line x = 27 mm), i.e. closer to the source (groundwater in the crack enclave). The slice Z4, representing material in the centre of the specimen, shows rather low area fractions close to the fracture plane. This could be explained by the restricted access of sulphide containing groundwater to this area (most of the sulphide would have been consumed in reactions with the outer parts of the crack flanges before the water reached the centre part).

It is also clear from the results that there must be some preferential paths within the microstructure for sulphur/sulphide entrance. For example, at location x=15 y=16 in slice Z4 a rather high area fraction of $9.5*10^{-4}$ is found, despite of the facts that the location is very far from the source of sulphur/sulphide and that the nearest neighbouring locations show very low area fractions.
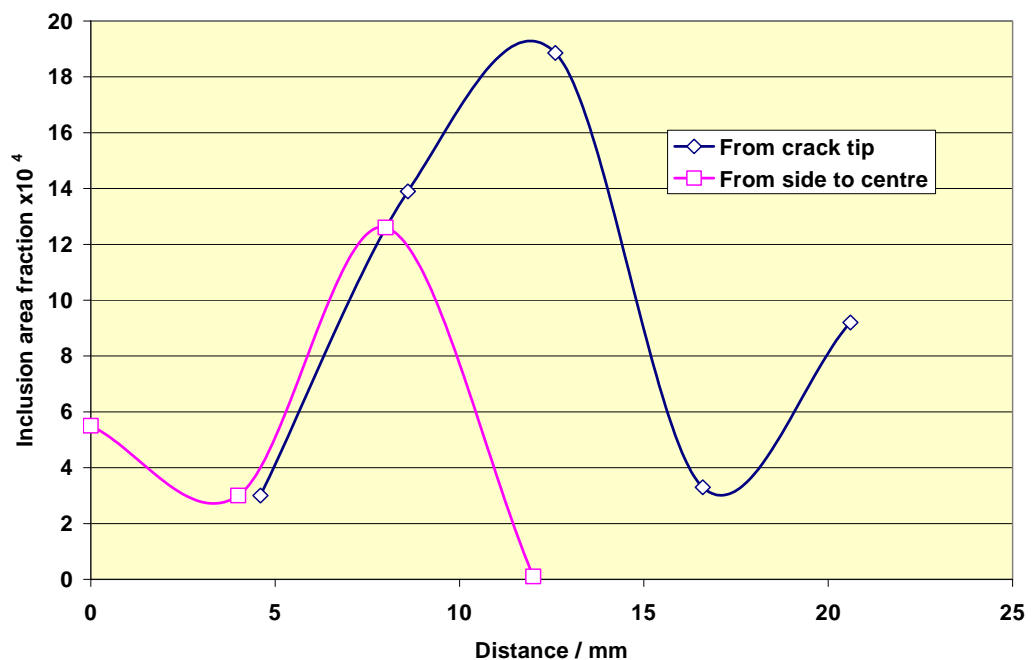

Figure 27. Area fractions of inclusions ($x10^4$) as a function of distance from the crack tip and from the side of the specimen.

Figure 27 shows the area fraction of inclusions as a function of distance from the crack tip (data from line x=27 mm in slice Z2), and from the side of the specimen towards the centre (one data point from each slice corresponding to the highest x- and y-values). This data can be basically compared with data gained by SEM/EDS on the fracture surface (shown in Fig. 20). Based on the comparison it would seem that the area fraction of inclusions increases and reaches a maximum at distances

where the sulphur concentration measured on the crack surface starts to decrease and reaches a minimum (see Fig. 20). This may indicate that precipitation of the inclusions causes the decrease in sulphur concentration. According to fracture mechanical calculations (Irwin's model) the size of the plastic zone ahead of the crack tip can be estimated as

$$r_p = \frac{(K_I)^2}{\pi(\sigma_{ys})^2}$$

where K_I is the stress intensity, about 9 MPam$^{0.5}$ in this case, and σ_{ys} is the yield strength, about 45 MPa for CuOFP at room temperature. Thus, the size of the plastic zone ahead of the crack tip in this case becomes $r_p = 12$ mm. This coincides rather well with the observed behaviour of sulphur in CuOFP, indicating that the presence of plastic deformation would tend to prevent precipitation of sulphur as inclusions.

4.6 Additional analysis of Test run 4

Test run 4 was performed in groundwater with 10 mg/l [S^{2-}]. The specimen was covered with lacquer except for the crack tip area (see Fig. 28). Inclusion analysis was performed only on the area not covered with lacquer.
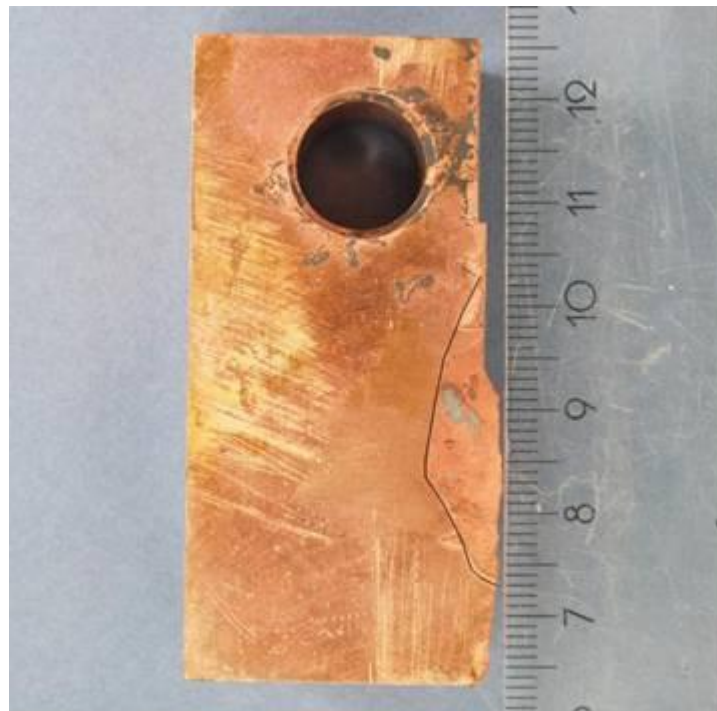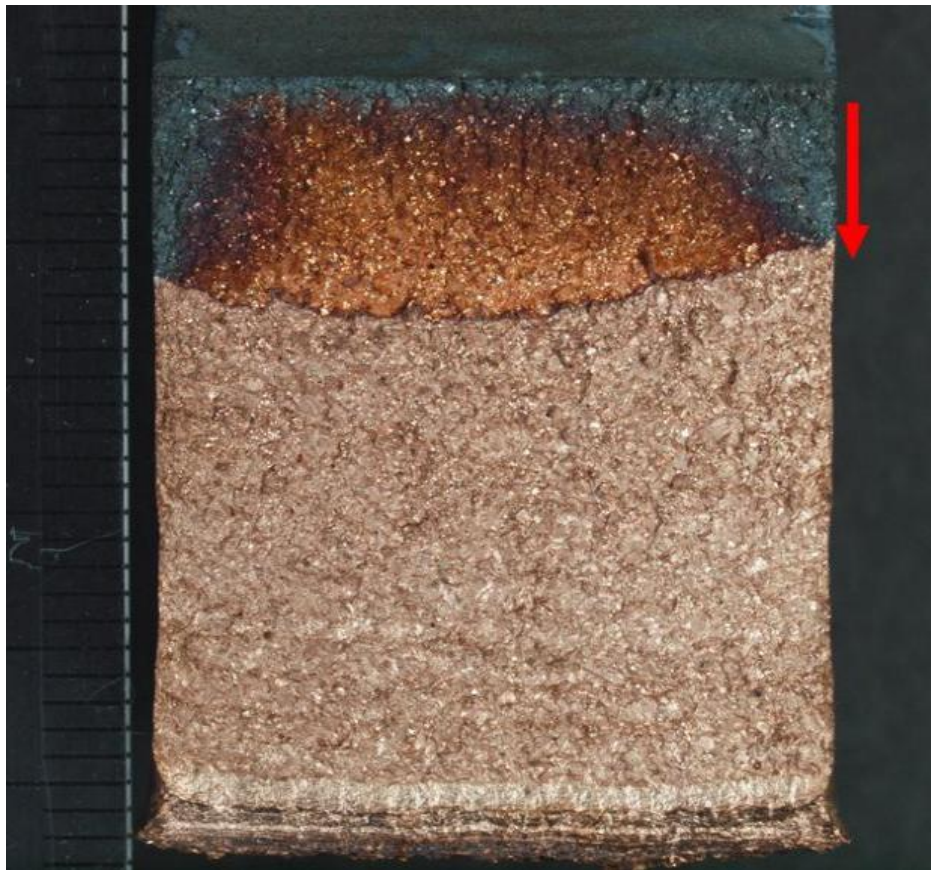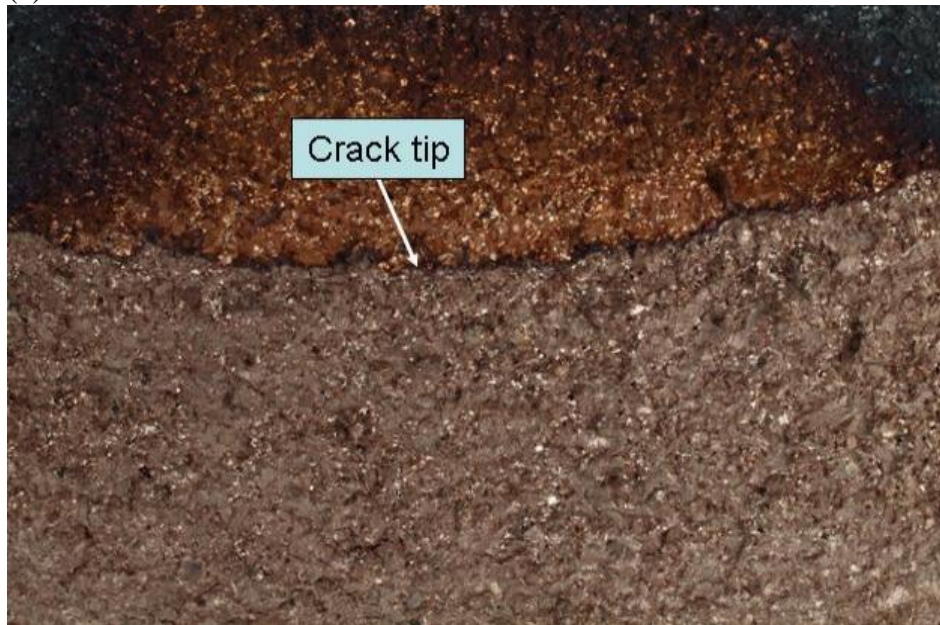

Figure 28. Side view of specimen 4 after the test. The black line contours the area that was not covered by lacquer during the exposure.

(a)

(b)

Figure 29. Fracture surface of specimen 4 after the exposure; general appearance (a) and detail (b).

From Fig. 29a it is clear based on the colour difference (which reflects a difference in film thickness) that the central part of the prefatigue area (red-brown colour) has not seen as much sulphide as the areas with shorter distance to the groundwater. This indicates that at this relatively low sulphide concentration most of the sulphide is consumed in reactions with those parts of the prefatigue area

more closer to the water, and the central area (due to restricted flow conditions) has been exposed to lower sulphide concentration. In the detail picture (29b), some small black spots could be detected ahead of the crack tip (more clearly visible directly under the microscope). The specimen was sliced in three parts so that the first surface was the outer surface of the specimen, the second one 6.25 mm and the third one 12.5 mm from the outer surface. Thus, the third slice represents the central part of the specimen. The image analysis for inclusions was performed using

Fig. 30 shows a comparison of un-exposed CuOFP and CuOFP exposed to groundwater with 10 mg/l [S^{2-}] for two weeks. In comparison to exposure to groundwater with 100 mg/l [S^{2-}] (see Fig. 22), the average size of inclusions is smaller and the number is larger.
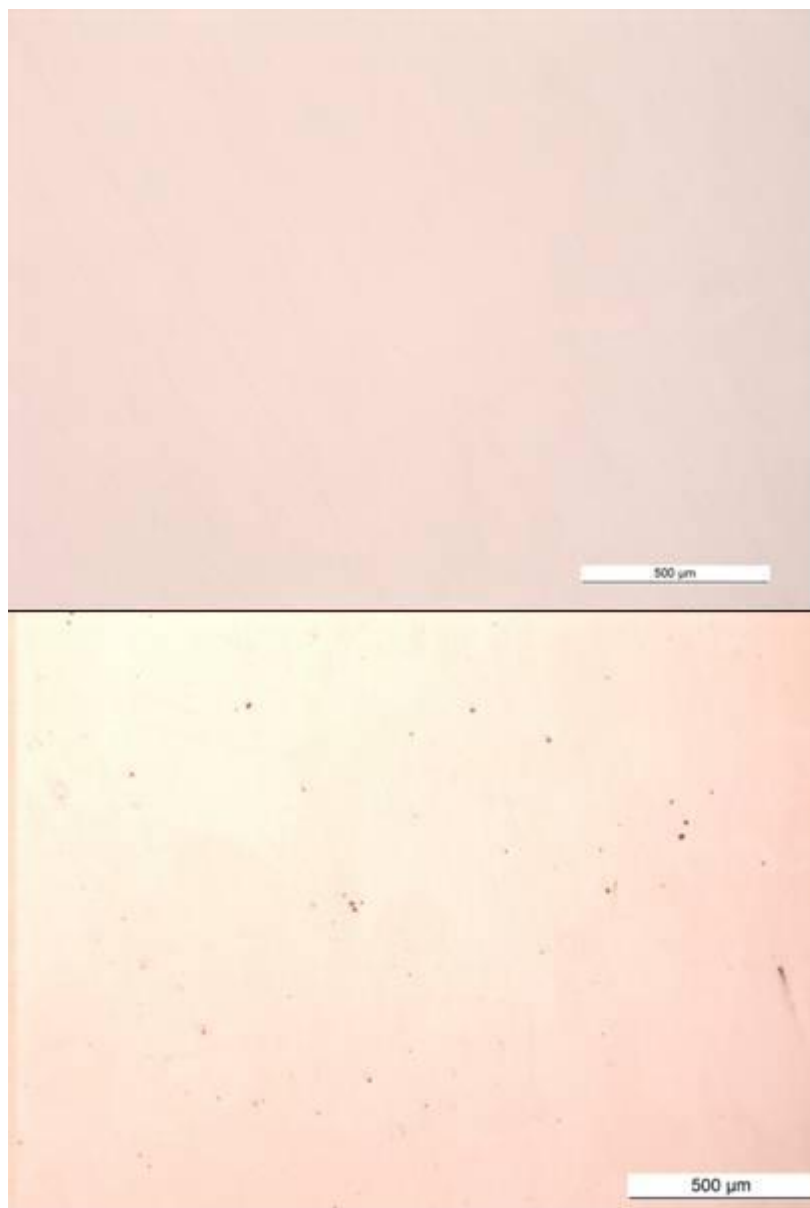

Figure 30. Comparison of polished surface of unexposed CuOFP and that of slice Z1 of specimen 4 (see below Fig. 31).
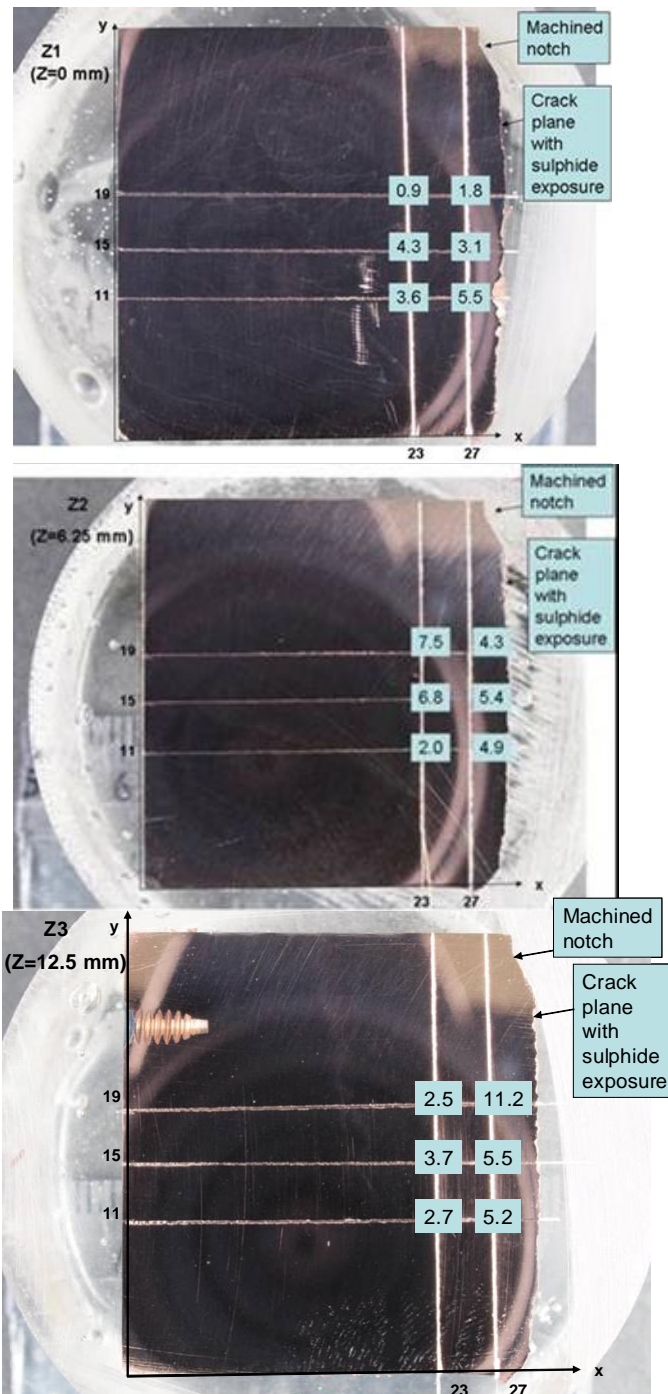
Figure 31. Area fractions of inclusions ($\times 10^4$) in specimen 4, slice Z1 (0 mm from outer surface, upper picture), slice Z2 (6.25 mm from outer surface, centremost picture), and slice Z3 (12.5 mm from outer surface, lowest picture), as a function of location.

The area fractions shown in Fig. 31 are surprisingly high, comparable to those found for the higher sulphide concentration (see Figs. 23 to 26). Based on these limited number of data it seems that the in-diffusion of sulphur/sulphide is possibly not directly related to the concentration of sulphide in the groundwater.

5 Task 4. Development of a sulphide diffusion in bentonite – model

In relation to this task, an attempt to determine the reaction rate constant for the reaction $2HS^- + 4Cu = 2Cu_2S + H_2 + 2e^-$ was made. A 10 l glass vessel was filled with groundwater, oxygen was removed by nitrogen bubbling and then 2 mg/l sulphide was added (as Na_2S). The sulphide concentration was monitored for three days using Hach Lange DR2800 spectrophotometer. This run constituted a "blank test". In the second phase, thin copper sheets with a total surface area of 5.5 cm^2 were installed into the glass vessel and the test procedure was repeated.

Fig. 32 shows the difference in sulphide consumption between the blank test and the one with copper sheets. Calculating for the volume (10 l) and surface area (5.5 cm^2 results in a reaction rate constant of

$$k = 2.3*10^{-7} \text{ gcm}^{-2}\text{s}^{-1}$$

It is noteworthy that according to the data in Fig. 32 the reaction is zero-order with regard to sulphide concentration, i.e. the reaction rate does not depend on the sulphide concentration (at least within the concentration range in this test, i.e. 2 mg/l to 0.5 mg/l). This may indicate that the rate of the reaction is determined by the surface reaction itself and not by e.g. diffusion of sulphide towards the surface. Also, the reaction product layer forming on the copper sheets, i.e. Cu_2S, seems not to be protecting as it does not have the ability to slow down the reaction rate. The reaction rate constant is roughly two orders of magnitude higher than the maximum flux estimated to arrive at the copper canister surface /3/. Thus, the diffusion rate of sulphide to the canister surface would always be expected to be rate limiting with respect to this reaction. The scenario used for the maximum flux estimation was as follows. Advective conduction through the bentonite was assumed (e.g. as a result of bentonite erosion) and the source sulphide concentration at the bentonite/rock interface was taken to be 450 mg/l [S^{2-}] (e.g. SRB population with unlimited flux of nutrients).
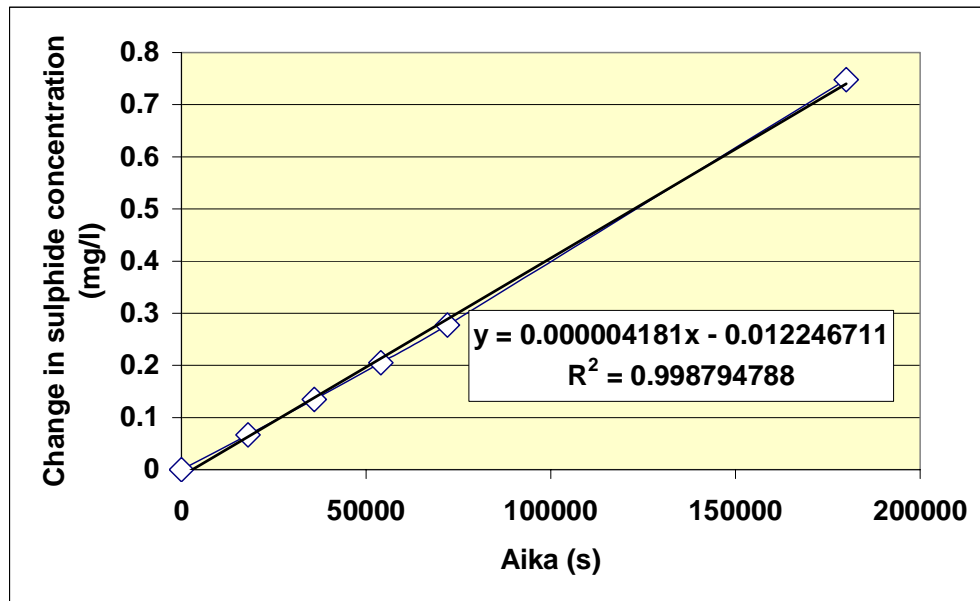
Figure 32. Difference in sulphide consumption as a function of time between a blank test and one with 5.5 cm^2 copper as thin sheets. Groundwater (10 l) with 2 mg/l sulphide.

6 Summary and conclusions

Precracked CT-specimens of CuOFP have been exposed to groundwater with 200 mg/l, 100 mg/l and 10 mg/l sulphide. On-line monitoring using the Potential Drop technique as well as displacement measurement of the specimen both indicated continuous changes in the material properties of CuOFP during the exposure. SEM/EDS studies of the fracture surface showed that during the exposure sulphur/sulphide had entered the material ahead of the precrack tip, with penetration rate of around 1 mm per week. Individual grain boundaries were found to contain above 20 at% sulphur. Optical metallography of sliced and polished cuts of exposed samples showed that sulphide inclusions could be found in all three dimensions of the material and not only in the crack plane. As a conclusion, the continuous changes in the on-line monitoring signals were attributed to the accumulation of sulphur/sulphide in the grain boundaries ahead of the precrack tip and further precipitation as inclusions.

Based on the results it is clear that sulphur can diffuse into the Cu OFP material when it is exposed at room temperature to saline groundwater with 10 to 200 mg/l sulphide. Indications were found that the in-diffusion preferentially occurs through grain boundaries and that high stress favours accumulation of sulphur/sulphide. Further investigations are needed to determine the effects of sulphur/sulphide in-diffusion on mechanical properties of CuOFP.

References

1. Taniguchi, N. and Kawasaki, M., 2008. Influence of sulphide concentration on the corrosion behaviour of pure copper in synthetic seawater. Journal of Nuclear Materials 379 (2008) 154-161.

2. Pedersen, K., 2010. Analysis of copper corrosion in compacted bentonite clay as a function of clay density and growth conditions for sulphate–reducing bacteria. Journal of Applied Microbiology, 108 (2010) 1094-1104.

3. Olin, M., 2010. Diffusion model for sulphide in compacted bentonite. VTT Research Report VTT-R- 00662-10.